

Power-law behaviour and parametric models for the size-distribution of forest fires

William J. Reed ^{a,*}, Kevin S. McKelvey ^b

^a Department of Mathematics and Statistics, University of Victoria, P.O. Box 3045, Victoria, BC, Canada V8W 3P4

^b Forestry Sciences Laboratory, USDA Forest Service, RMRS, P.O. Box 8089, Missoula, MT 59807, USA

Received 13 February 2001; received in revised form 6 November 2001; accepted 6 November 2001

Abstract

This paper examines the distribution of areas burned in forest fires. Empirical size distributions, derived from extensive fire records, for six regions in North America are presented. While they show some commonalities, it appears that a simple power-law distribution of sizes, as has been suggested by some authors, is too simple to describe the distributions over their full range. A stochastic model for the spread and extinguishment of fires is used to examine conditions for power-law behaviour and deviations from it. The concept of the extinguishment growth rate ratio (EGRR) is developed. A null model with constant EGRR leads to a power-law distribution, but this does not appear to hold empirically for the data sets examined. Some alternative parametric forms for the size distribution are presented, with a four-parameter ‘competing hazards’ model providing the overall best fit. © 2002 Elsevier Science B.V. All rights reserved.

Keywords: Fire area; Power-law; Size distribution; Extinguishment growth rate ratio; Self-organized criticality

1. Introduction

A number of recent papers have examined the size-distribution of wildfires (Malamud et al., 1998; Ricotta et al., 1999; Cumming, 2001). In all three cases, the claim has been made that empirical size-distributions exhibit power-law behaviour. In the first two papers, it is argued that the observed power-law behaviour is consistent with

the self-organized criticality (SOC) arising in simple dynamical systems models. Malamud et al. argue for power-law behaviour from what physicists call the ‘forest-fire model’ (Bak et al., 1990) while Ricotta et al. use the ‘sandpile model’ (Bak et al., 1988) as a metaphor. In contrast Cumming makes no claim based on theory—only that the best-fitting parametric distribution that he can find is a truncated exponential distribution for the logarithm of area or, in other words, a truncated power-law (or Pareto) distribution for area. An earlier paper (Baker, 1989) claims that the size-distribution is exponential. In this article, we first examine whether evidence from fire records supports a single form for the size distribution and, if

* Corresponding author. Tel.: +1-250-721-7469; fax: +1-250-721-8962.

E-mail addresses: reed@math.uvic.ca (W.J. Reed), kmckelvey@fs.fed.us (K.S. McKelvey).

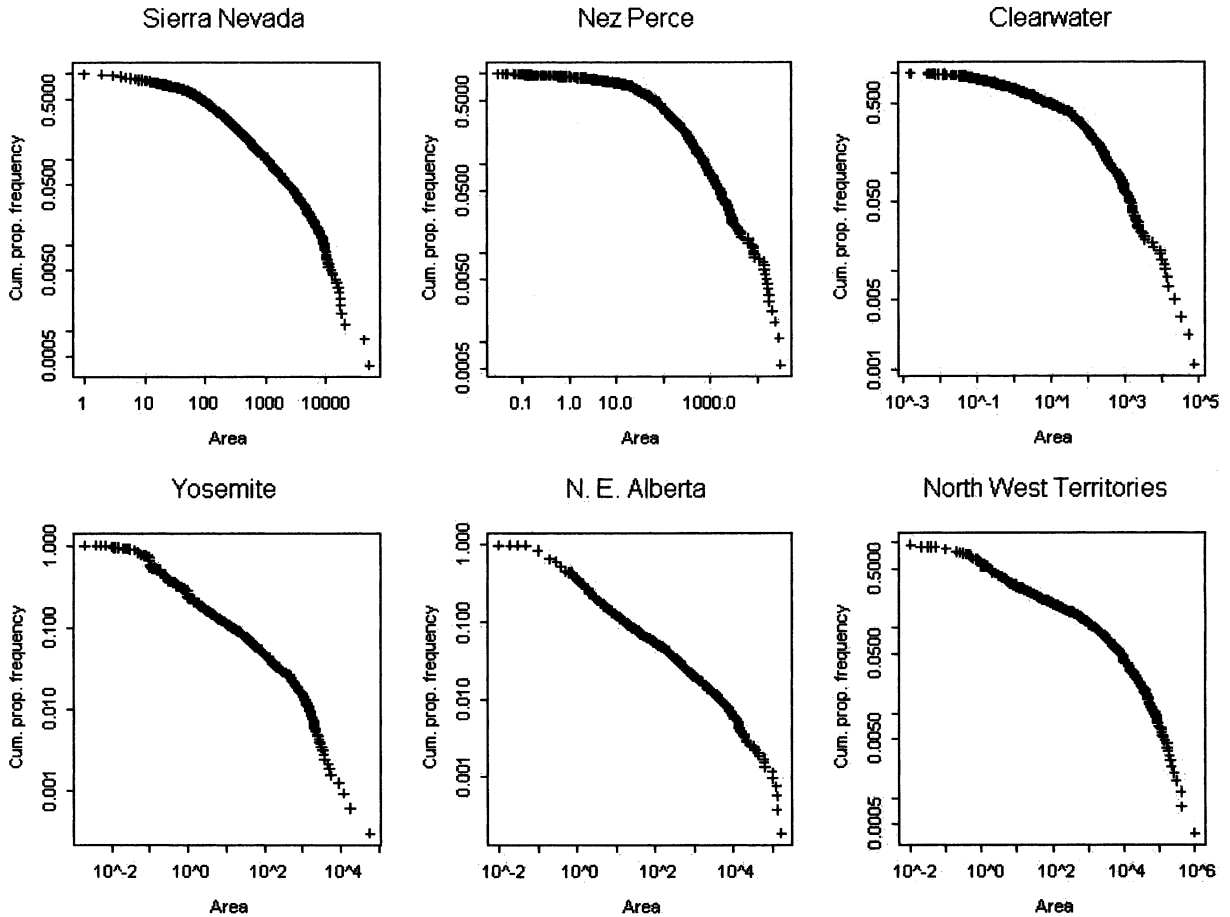


Fig. 1. Cumulative frequency plots (empirical survivor functions) with logarithmic axes for the size distribution of areas burned for the six datasets described in Section 2. Area is measured in hectares.

so, whether it could be as simple as a power law. We then examine conditions for power-law behaviour using a simple stochastic process model for the growth and extinguishment of fires. Finally, we offer some new parametric forms for the size distribution and discuss their properties and fit.

2. Empirical fire size distributions

Fig. 1 shows logarithmic cumulative frequency plots, i.e. plots of the cumulative proportion of all fires (ordinate) as big or bigger than a given level (abscissa), with both axes on logarithmic scales

for six sets of data¹. Fig. 2 shows plots of a nonparametric estimate (Silverman, 1986) of the density (plotted on logarithmic scale) for the logarithm of area for the same six data sets. Even though there are some differences (e.g. between

¹ 2536 fires in Sierra Nevada US Forest Service Land, 1908–1992 (McKelvey and Busse, 1996); 1795 fires in Nez Perce National Forest, 1870–1994; 884 forest in Clearwater National Forest, 1910–1992; 3190 fires in Yosemite National Park, 1930–1999 (all unpublished USDA Forest Service data); 5478 forest in N.E. Alberta 1961–1998 (Alberta Environment. Forest protection webpage <http://www.gov.ab.ca/env/forest/fpd>) and 2544 fires in Northwest Territories, 1992–1999 (Northwest Territories Department of Resources, Wildlife and Economic Development webpage <http://216.108.146.3/Fires/Fires%20Archive/firesarchive.htm>).

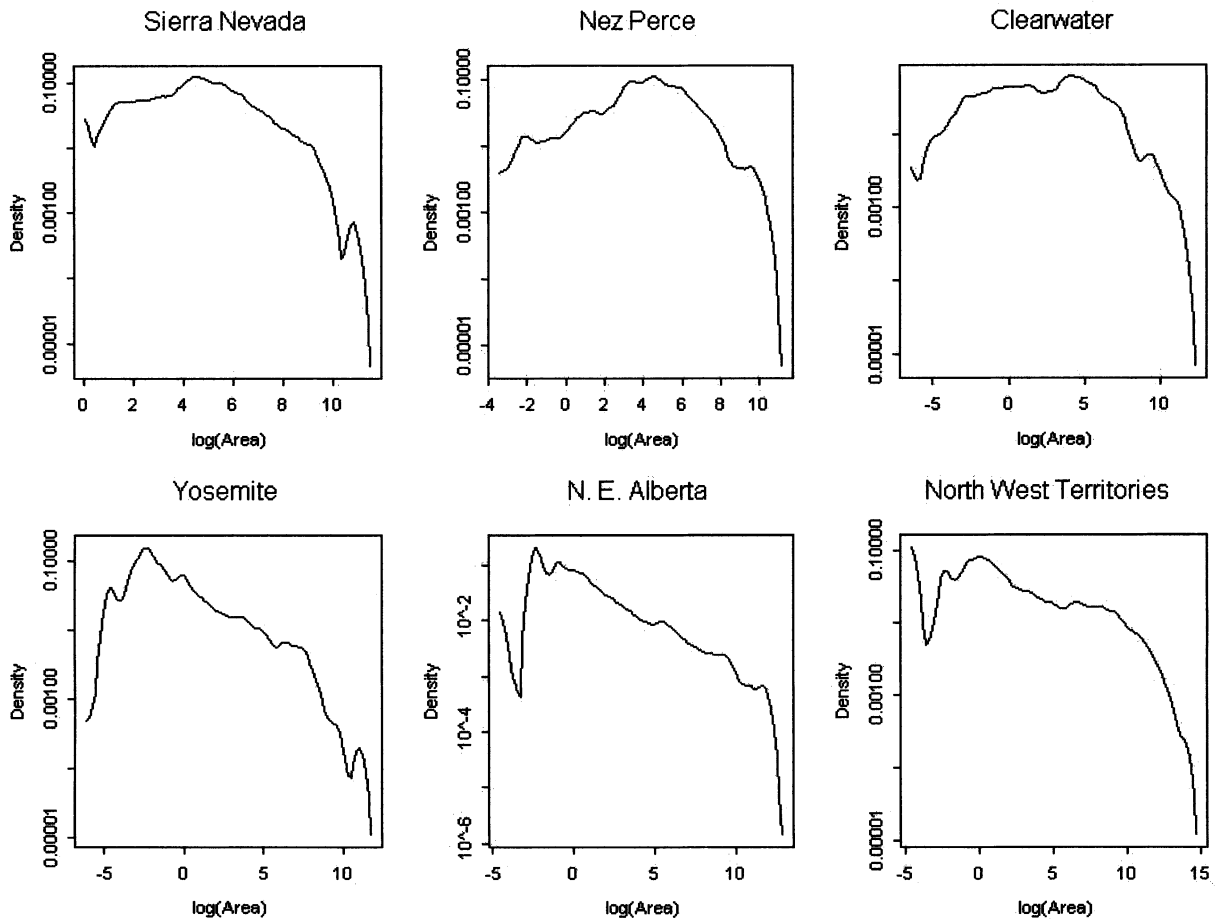


Fig. 2. Nonparametric estimates of the density for the distribution of the natural logarithm of areas burned for the six datasets described in Section 2.

the plots in the top row and those in the bottom row), there are enough similarities to suggest the possibility of them following a single parametric form. Could this form be as simple as a power law (Pareto distribution) as claimed by some authors?

If X is a random variable denoting area, with its probability density function (pdf) following a power law (or Pareto) distribution, i.e. $f_X(x) \propto x^{-a}$, then $S(x) = P(X \geq x) \propto x^{-a+1}$ and $\log S(x) = c_1 - (a-1)\log(x)$. Thus, if there is power-law behaviour, the plots in Fig. 1 should each contain points close to a straight line of negative slope. Also the pdf of $Y = \log(X)$ is $f_Y(y) \propto \exp(-(a-1)y)$, so that $\log f_Y(y) = c_2 - (a-1)y$ and the plots in Fig. 2 should also con-

tain points close to a straight line. Clearly this is not the case, although there is evidence of straight line behaviour (and thus power-law behaviour in the underlying distribution) over a limited range of sizes, e.g. for the middle range for N.E. Alberta and Yosemite data sets.

The cumulative frequency plot presented by Ricotta et al. (1999) for fires in Liguria, Northern Italy, has a similar form to those in Fig. 1. Those authors offered an explanation for what they claimed was power law behaviour in the empirical distribution. However, it was only after they had removed approximately the largest 1.5% fires (those bigger than 100 ha) and the smallest 50% of all fires (those smaller than 1 ha) that some-

thing approximating a straight line plot could be obtained. Similar data massaging (eliminating unwanted points) could produce straight line plots over a limited range, at least for the N.E. Alberta and Yosemite data.

In the next section, we present a simple stochastic process model for the growth and extinguishment of fires and use it to determine conditions for power-law behaviour.

3. A model for the process determining fire size

Wildfires share with many biological entities the fact that they grow in time in a monotonic and stochastic way and also die in a stochastic way. A realistic mathematical model should include both of these aspects, i.e. it should include a monotone stochastic process with a stochastic stopping ('killing' or extinguishment) rule.

The growth of a fire is a very complicated affair, depending on weather, topography, fuel types and other factors. It is difficult to include all such factors in a simple model, but since we are concerned only with the final area of the fire, we need only be concerned with the growth, in time, of the area burned. We shall do this by specifying the growth in area burned as a stochastic process, ignoring shape and other spatial aspects. It seems reasonable to assume that growth is size-dependent, i.e. that the rate of growth in area depends on the current area. For example, for an idealized disk-shaped fire on flat homogeneous terrain, with its front moving outwards at a constant velocity, the rate of growth in area is proportional to the square root of area. For more general size-dependent stochastic growth, we seek a monotone stochastic process which generalizes the ordinary differential equation (o.d.e.)

$$\frac{dX}{dt} = \mu(X),$$

with $\mu(X) \geq 0$. A stochastic differential equation (sde) version of this will not provide a good model because sample paths of sdes are not monotone. As an alternative, we consider a pure birth process model (e.g. Tuckwell, 1988), in continuous time but with discrete states, labeled 1, 2, 3, . . .

etc. These states can be defined in terms of 'marker sizes' x_1, x_2, x_3, \dots etc. (e.g. at levels 1, 2, 3, . . . ha; or 1, 2, 3, . . . m²) with the process considered to be in state j at time t if the area $X(t)$ burned by that time, exceeds marker size x_j , but not marker size x_{j+1} (i.e. $x_j < X(t) \leq x_{j+1}$). For simplicity, we shall suppose that the marker sizes are equally spaced so that $x_{j+1} - x_j \equiv \Delta$, for all j . Let

$$\lambda_j = \frac{\mu(x_j)}{\Delta}$$

and suppose that if the process is in state j at time t , the probability of it being in state $j+1$ an infinitesimal time later, at time $t+dt$, is $\lambda_j dt + o(dt)$; the probability of it still being in state j is $1 - \lambda_j dt + o(dt)$; and the probability of it being in some higher state is $o(dt)$. For this process, the expected growth in size in the infinitesimal interval $(t, t+dt)$ given $X(t) = x_j$ is

$$\begin{aligned} E(X(t+dt) - X(t) | X(t) = x_j) &= \lambda_j \Delta dt + o(dt) \\ &= \mu(x_j) dt + o(dt), \end{aligned}$$

so that

$$E(dX | X(t)) = \mu(X(t)) dt + o(dt),$$

which provides a stochastic generalization of the o.d.e. model above.

Also, from standard birth-death process results, the expected time to grow from state j_0 to j_1 is

$$\sum_{i=j_0}^{j_1} \frac{1}{\lambda_i} = \sum_{i=j_0}^{j_1} \frac{\Delta}{\mu(x_i)}$$

If $\Delta \rightarrow 0$, the above sum converges to

$$\int_{X_0}^{X_1} \frac{dy}{\mu(y)}$$

(where X_0 and X_1 are the sizes corresponding to j_0 and j_1) which is the time to grow from level X_0 to level X_1 in the deterministic model $dX/dt = \mu(X)$. Thus, for a fine mesh (Δ small), our model can be regarded as being a stochastic growth model, which generalizes the o.d.e. model.

To illustrate the growth model, consider the simple case with a constant expected proportional growth rate, i.e. with $\mu(X) = \mu X$ (μ a constant). In this case, $\lambda_j = \mu(x_j)/\Delta = j\mu$ and the process is a homogeneous pure birth (or Yule) process (e.g.

Tuckwell, 1988), a stochastic version of exponential growth, with $E(X(t)) = X_0 e^{\mu t}$ and $\text{var}(X(t)) = X_0 e^{2\mu t}(1 - e^{-\mu t})$.

The extinguishment of the fire needs to be modelled stochastically. This can be carried out mathematically using a ‘killing rate’ function

$$k(t) = \lim_{dt \rightarrow 0} \frac{1}{dt} P(T < t + dt | T > t),$$

where T is the time of extinguishment or ‘killing’. Typically, the probability of extinguishment will be size-dependent, with, other things being equal, a big fire being less likely to go out than a small fire. Thus, we shall assume that

$$k(t) = v(X(t))$$

where $v(x)$ is a non-increasing function. Let $v_j = v(x_j)$, $j = 1, 2, \dots$, so that the probability of the fire going out in the infinitesimal interval $(t, t + dt)$, given that it was in size class j at time t is $v_j dt + o(dt)$. We shall refer to $v(x)$ as the extinguishment rate.

With these assumptions, the final size (the size of the fire when extinguishment occurs) can be determined from a more general result of Berman and Frydman (1996). Let \bar{X} denote the state when the process is killed. Then

$$\begin{aligned} f_j = P(\bar{X} = j) &= \frac{v_j}{v_j + \lambda_j} \prod_{i=1}^{j-1} \frac{\lambda_i}{\lambda_i + v_i} \\ &= \frac{\rho_j \Delta}{1 + \rho_j \Delta} \prod_{i=1}^{j-1} \frac{1}{1 + \rho_i \Delta} \end{aligned} \tag{1}$$

where

$$\rho_j = \frac{v_j}{\Delta \lambda_j} = \frac{v_j}{\mu(x_j)}.$$

Note that we can write

$$f_j = \theta_j \prod_{i=1}^{j-1} (1 - \theta_i),$$

where

$$\theta_j = \frac{v_j}{v_j + \lambda_j} = \frac{\rho_j \Delta}{1 + \rho_j \Delta}.$$

In this form, it is clear that θ_j constitutes a discrete hazard function, being the probability of

extinguishment in size-class j , given that the process has reached that class. The product $\prod_{i=1}^{j-1} (1 - \theta_i)$ constitutes a survivor function (i.e. it equals $P(\bar{X} \geq j)$). If it converges (as $j \rightarrow \infty$) to a positive value, there is a non-zero probability of the process never being killed. In this case, the distribution of \bar{X} is improper, having a non-zero probability at infinity.

We can get a similar result passing to the continuum limit, i.e. dividing by Δ and then letting $\Delta \rightarrow 0$, yields a density for \bar{X} of the form

$$f_{\bar{X}}(x) = \rho(x) \exp\left(-\int_{x_0}^x \rho(x') dx'\right) \tag{2}$$

where $\rho(x) = (v(x)/\mu(x))$. Here, $\rho(x)$ is the hazard rate function (i.e. $\rho(x)dx$ represents the probability that \bar{X} is less than $x + dx$ given that it exceeds x). The corresponding survivor function is

$$S_{\bar{X}}(x) = P(\bar{X} \geq x) = \exp\left(-\int_{x_0}^x \rho(x') dx'\right) \tag{3}$$

Eq. (2) and Eq. (3) both describe the distribution of final fire size in the model. The empirical cumulative distributions plotted in Fig. 1 are sample equivalents of $S_{\bar{X}}(x)$ in Eq. (3).

3.1. Conditions for power-law behaviour

Power-law behaviour in the distribution of fire size is represented by straight-line behaviour in the plot of $\log S_{\bar{X}}(x)$ vs. $\log x$. If the density $f_{\bar{X}}(x)$ is changing faster (respectively slower) than a power-law, then there will be concavity (respectively convexity) in the plot of $\log S_{\bar{X}}(x)$ vs. $\log x$. For the density to behave asymptotically like a power law, $\log S_{\bar{X}}(x)$ must be asymptotically linear in $\log x$.

The concavity/convexity of the plot of $\log S_{\bar{X}}(x)$ vs. $\log x$ can be determined from the ratio of extinguishment rate $v(x)$ to the proportional expected growth rate in area $\mu(x)/x$. We shall call this the extinguishment-growth-rate ratio (EGRR) and write it

$$\text{EGRR} = \frac{xv(x)}{\mu(x)} = R(x).$$

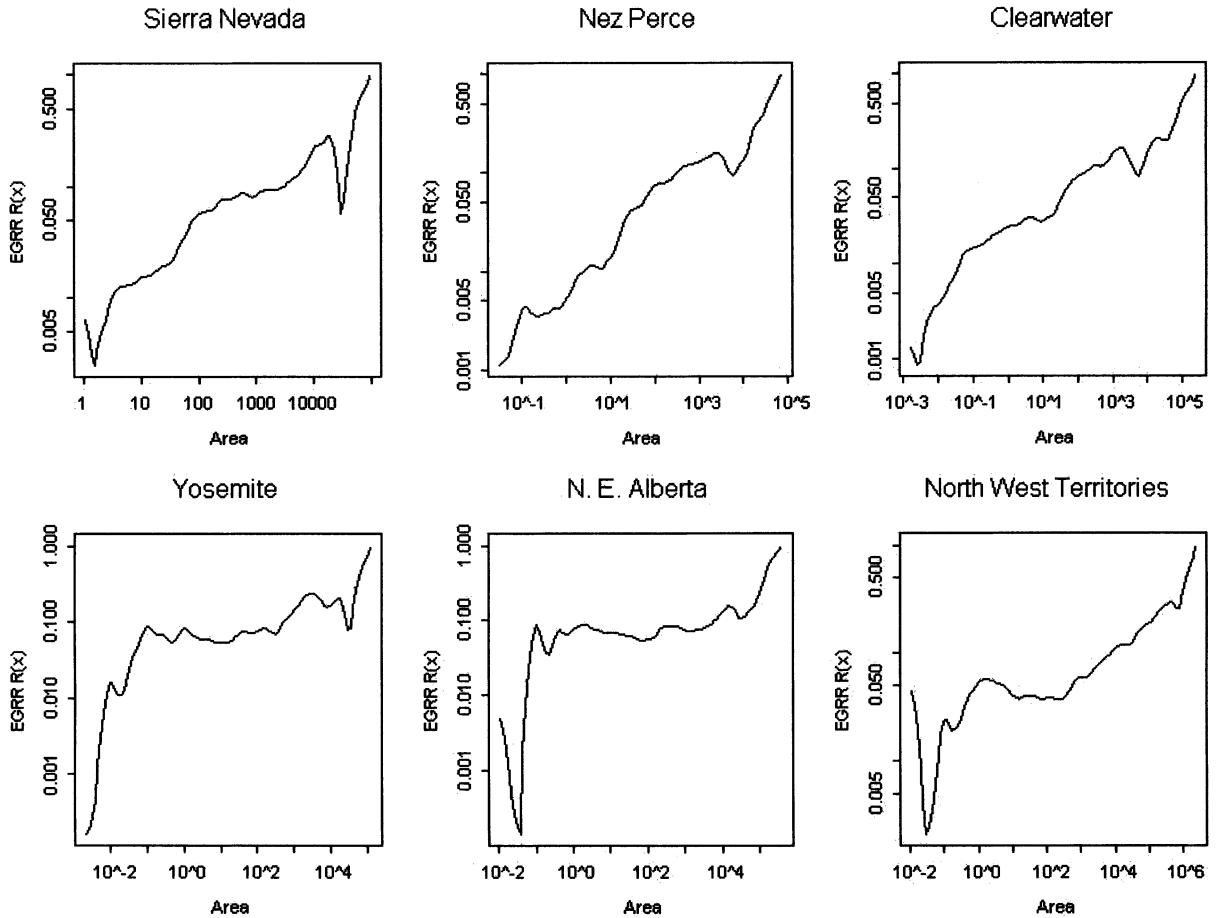


Fig. 3. Nonparametric estimates of the extinguishment growth rate ratio (EGRR) derived from the density estimates in Fig. 2, for the six datasets described in Section 2.

In Appendix A, it is shown that the EGRR is related to the pdf $f_{\bar{X}}(x)$ and the survivor function $S_{\bar{X}}(x)$ of the final size \bar{X} by

$$R(x) = \frac{x f_{\bar{X}}(x)}{S_{\bar{X}}}, \text{ say.}$$

and that this is the negative slope of the graph of $\log(S_{\bar{X}}(x))$ vs. $\log x$. This means that a non-parametric estimate of the EGRR can be found from a histogram-based estimate of the density (e.g. Silverman, 1986), as in Fig. 2. Fig. 3 shows such estimates (both EGRR and area on logarithmic scales) for the six data sets introduced in Section 2. They all follow rather similar forms.

Clearly, for there to be power-law behaviour on an interval, the EGRR must be constant on that interval (so that $\log S_{\bar{X}}(x)$ is linear in $\log x$ there). On the other hand, if the EGRR is increasing over an interval, the graph of $\log S_{\bar{X}}(x)$ vs. $\log x$ will be concave there and the distribution of \bar{X} will be changing faster than a power-law; while if the EGRR is decreasing, the graph will be convex and the distribution of \bar{X} changing more slowly than a power-law.

Thus, power law behaviour will occur at intervals where the EGRR is constant. This can be seen empirically by observing in Fig. 3 that the estimated EGRR is approximately constant in the middle range for the Yosemite and N.E. Alberta

data. This corresponds to approximately linear behaviour in the corresponding panels of Fig. 1 and Fig. 2.

Power-law behaviour over the whole range of sizes, as for example claimed by Malamud et al. (1998), requires that the EGRR be constant at all sizes or, in other words, that at all times and sizes, the probability of the fire being extinguished (in an infinitesimal time interval of length dt) be a constant multiple of the expected increment in size (as a proportion of current size) in the infinitesimal time interval, given that the fire is not extinguished. This is a highly restrictive condition and there seems to be no obvious reason why it should hold.

A more limited form of power-law behaviour is that it should occur asymptotically in the upper-tail of the distribution, i.e. $f_{\bar{X}}(x) \sim x^{-\alpha-1}$ and $S_{\bar{X}}(x) \sim x^{-\alpha}$ as $x \rightarrow \infty$ ². It is shown in Appendix A that a necessary and sufficient condition for upper-tail power-law behaviour is that the EGRR converges to a positive limit, as $x \rightarrow \infty$.

A weaker form of upper-tail power-law behaviour can occur when $R(x) \rightarrow 0$ as $x \rightarrow \infty$. It is shown in Appendix A that, in this case, the distribution of \bar{X} is improper, i.e. $S_{\bar{X}}(x) \rightarrow S_{\infty} > 0$ so that there is a nonzero probability that \bar{X} is infinite. A fire of infinite extent is of course an artifact of the model and can never occur in practice. This leads naturally to the question of where the model fails to reflect reality. We see at least two simplifications made in the model which relate to this. The first is that there is no upper bound on the variable X , whereas in reality there is an upper limit on fire size imposed by geography, e.g. trivially by the area of the continent in which it occurs. Secondly, the model is time-homogeneous, and neglects factors such as a change in the seasons. Sometimes large fires are extinguished only when summer ends and autumn precipitation occurs, as for example with fires in Montana in 2000. This is hard to model and is not included explicitly in our model. One can confine their attention to finite fires by condition-

ing on the event that \bar{X} is finite. The conditional distribution of \bar{X} , given that \bar{X} is finite, can exhibit asymptotic power-law behaviour. In Appendix A it is shown that this will occur if and only if $R(x) \sim x^{-\alpha}$ for some $\alpha > 0$. Figs. 1–3 suggest that no form of upper-tail power-law behaviour occurs for any of the six data sets under study.

3.2. A special case

Consider the plausible special case in which the growth function is of the form $\mu(X) = c_0 X^{1-b}$ where $0 \leq b \leq 1$, with the extreme cases corresponding to exponential growth ($b = 0$) and linear growth ($b = 1$). Intermediate cases could be quite important. To see this, consider a highly idealized fire which maintains a fixed shape (e.g. a circular fire, or an elliptical fire, with ratio of major and minor axes remaining constant). If such a fire were to grow outward with the front moving at a fixed velocity, its area X , say, would grow according to $dX/dt = cX^{1/2}$, so that X would scale with t^2 . If the shape of the fire was not regular, but instead a fractal with its area related to a length dimension L by a power-law relationship $X \propto L^{1/b}$ $0 < b < 1$ and the length dimension was growing at a fixed velocity (front moving at fixed velocity), then $dX/dt \propto X^{1-b}$ and X would scale as $t^{1/b}$. The stochastic versions of this model could allow for irregularities in fuel, topography, wind etc. Indeed repeated simulations of a simple percolation model for the spread of a fire in a homogeneous forest suggest that the mean area burnt t time steps after initiation, scales as t^β with $\beta > 1$, lending support to this model form. The EGRR for the special case is $R(x) = x^b v(x)$. This is constant on an interval (leading to power-law behaviour there) only if $v(x) \propto x^{-b}$ on the interval; and tends to a positive limit (leading to upper-tail power law behaviour) only if $v(x) \sim x^{-b}$. It would seem to be only through a fluke that such conditions could hold. However, conditional³ upper-tail power-law behaviour could occur under slightly less restrictive conditions, namely when $v(x) \sim x^{-b-\varepsilon}$, with $\varepsilon > 0$.

² We use the standard notation for asymptotic equivalence, i.e. $f(x) \sim g(x)$ as $x \rightarrow \infty$ indicates $\lim_{x \rightarrow \infty} (f(x)/g(x))$ exists and is strictly positive.

³ Asymptotic power-law behaviour in the distribution of size condition on it being finite, as described in Section 3.1.

There is a particularly interesting case in which full power-law behaviour would occur. This is when both the growth rate and the extinguishment rate are independent of size, i.e. where there is stochastic exponential growth ($\mu(x) \propto x$) and a constant extinguishment probability ($v \equiv \text{constant}$). In this case, the EGRR is constant and a power-law distribution would result. We can think of this as a null model and examine how growth and extinguishment rates might deviate from constant, null values. Firstly, a size-independent extinguishment rate seems unlikely, in that other things being equal, a big fire would probably be less likely to go out due to a given rainstorm etc., than a small fire. Similarly, exponential growth in fire size seems unlikely. For example, for a circular fire spreading outwards, exponential growth in area would require the velocity of the front to increase exponentially in time. Considerations such as these would suggest that both the expected proportional growth rate and the extinguishment probability to decline with size. Whether their ratio should increase or decrease is not obvious. The empirical plots of the EGRR (Fig. 3) suggest that it increases with size, and thus that, overall, the pdf of fire size $f_{\bar{x}}(x)$ should decay with x faster than a power law.

3.3. Multiple causes of extinguishment

It is difficult to decide theoretically on the behaviour of the EGRR. However, some thought about the causes of extinguishment may help shed some light. Extinguishment of a small fire could come about because of lack of fuel in surrounding areas. For a fire to go out for this reason, it would need to go out everywhere on its boundary, the length of which is likely to be related to area through a power-law relationship. Thus a reasonable model for the extinguishment rate from this cause might be of the form $c \exp(-\lambda x^a)$, ($c, \lambda, a > 0$). Note that this becomes small quite rapidly as x increases. Another cause of extinguishment is precipitation. Several days of heavy rainfall could extinguish a fire of any size, but lesser precipitation might only be sufficient to extinguish smaller fires, with its effect on larger fires being to slow the growth. Thus, it seems that a reasonable model for the extinguishment rate due to rainfall could be of

the form $\pi(x)$, where π is a decreasing function, decreasing more slowly than the previous term. Another cause of extinguishment could be intervention by fire-fighting crews. This is hard to model, since proximity to human settlements, commercial value of the standing timber etc., are likely to be the major determinants of the extent of fire-fighting efforts. However many people involved in fire fighting believe that suppression cannot put out very large fires. The effect of suppression efforts on such fires is more likely to be in reducing the spread (e.g. by putting lines around the back and sides of fires) rather than in actually extinguishing the fires. In this respect, the effect of suppression could be thought of as being similar to that of rainfall. Because of this, we will not model extinguishment through suppression separately, but rather consider the term $\pi(x)$ to cover both precipitation and suppression.

Combining these competing causes gives an overall extinguishment rate of the form

$$v(x) = c \exp(-\lambda x^a) + \pi(x)$$

and an EGRR of the form

$$R(x) = c_1 \frac{x \exp(-\lambda x^a)}{\mu(x)} + c_2 \frac{x\pi(x)}{\mu(x)}.$$

If $\mu(x) \propto x^b$, the first term will decay with x beyond a certain point. Whether the second term increases or decreases depends on how fast $\pi(x)$ declines compared with $\mu(x)/x$. The plots of non-parametric estimates of the EGRR in Fig. 3 suggest that, in all cases, the EGRR increases, beyond the very smallest sizes. This is true even for the Northwest Territories, where many fires are not actively combated, which suggests that the second term ($x\pi(x)/\mu(x)$), increases with size.

4. Some parametric forms for the distribution of area

In this section, we present three parametric forms for the distribution of area. They have been derived by examining the plots of nonparametric estimates of the EGRR in Fig. 3 and of the hazard rate $\rho(x)$ in Fig. 4, as well as the theoretical discussion above.

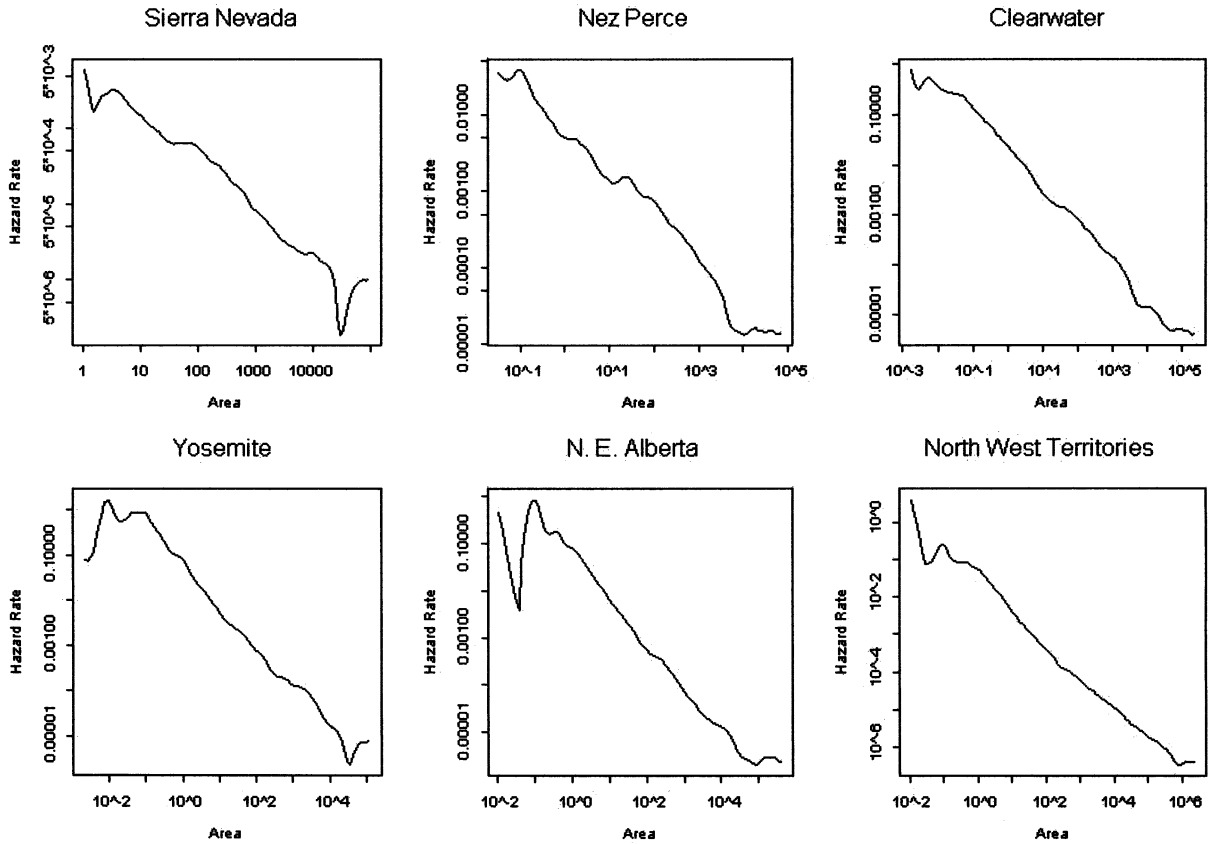


Fig. 4. Nonparametric estimates of the hazard rate function, derived from the density estimates in Fig. 2, for the six datasets described in Section 2.

4.1. Model I—Weibull (two parameters)

The plots of the nonparametric estimates of the hazard rate in Fig. 4, suggest approximately a linear relationship, when both hazard and area are in logarithmic scales. This suggests a hazard rate of the form

$$\rho(x) = ax^{-b},$$

with $b > 0$ which, at least for $b < 1$, is a Weibull hazard. The corresponding pdf is

$$f_{\bar{X}}(x) = ax^{-b} \exp\left\{-\frac{a}{1-b}(x^{1-b} - x_0^{1-b})\right\}$$

where x_0 is the minimum observable size for a fire. The EGRR is $R(x) = ax^{1-b}$, so that power-law behaviour would occur everywhere if $b = 1$, and

nowhere if $b < 1$. For $b > 1$, asymptotic power-law behaviour for the distribution of \bar{X} , conditional on \bar{X} being finite, would occur.

The model can be fitted by maximum likelihood under the assumption of independent observations⁴. The log-likelihood for n such observations (x_1, x_2, \dots, x_n) from the above distribution is

⁴ Even if the observations are not independent, the procedure of maximizing the log-likelihood can be justified as providing maximum likeness estimates (Barndorff-Nielsen, 1977), i.e. estimates which minimize the discrimination information between the distribution of the data and the fitted distribution.

$$\ell_1(a,b)$$

$$= n \log a - b \sum_{i=1}^n x_i - \frac{a}{1-b} \left(\sum_{i=1}^n x_i^{1-b} - nx_0^{1-b} \right)$$

This can be maximized analytically with respect to a , yielding

$$\hat{a} = \frac{n(1-b)}{\sum_{i=1}^n x_i^{1-b} - nx_0^{1-b}},$$

which when substituted into ℓ_1 yields a ‘concentrated’ (or profile) log-likelihood

$$\hat{\ell}_1(b) = n \log(1-b) - n \log \left(\sum_{i=1}^n x_i^{1-b} - nx_0^{1-b} \right) - b \sum_{i=1}^n \log x_i.$$

This can be maximized numerically with respect to b to yield maximum likelihood estimates (MLEs) of b and then of a . Table 1 shows these estimates and the corresponding maximized log-likelihood for the six data sets, in each case using the smallest observed fire as the value for x_0 .

The goodness of fit of the model can be assessed by examining Q–Q (quantile–quantile) plots of the observed and fitted distributions. These are displayed in Fig. 5 (both axes logarithmic). The fit appears to be satisfactory for the three data sets in the top row, but a little less satisfactory for those in the bottom row. Note however that the deviation from the 45° line is in a different direction for the Northwest Territories data, than for Yosemite and N.E. Alberta.

Table 1

Maximum likelihood estimates of the two parameters (a and b) of the Weibull model (Model I) with the corresponding maximized log-likelihoods

	\hat{a}	\hat{b}	$\hat{\ell}$
Sierra Nevada	0.0523	0.583	–33 928.84
Nez Perce	0.0489	0.554	–22 783.08
Clearwater	0.110	0.723	–9274.02
Yosemite	0.301	0.792	–26 910.61
N.E. Alberta	0.279	0.815	–53 130.46
North West Territories	0.163	0.878	–27 384.24

In the latter two cases, the fitted quantiles at the upper end of the distribution are too large, whereas for the Northwest Territories data, they are too small.

4.2. Model II—competing hazards (four parameters)

As discussed in Section 3.3, a fire may go out for a number of reasons. The probability of extinguishment due to lack of fuel will likely decrease quite rapidly with size, while extinguishment due to rainfall may decrease more slowly. To model this, one can consider a hazard rate with two components, declining at different rates. To this end consider a hazard rate of the form

$$\rho(x) = ax^{-b} + ce^{-dx}$$

which has a pdf

$$f_{\bar{x}}(x) = a(x^{-b} + \theta e^{-dx}) \exp \left\{ -a \left[\frac{x^{1-b} - x_0^{1-b}}{1-b} - \frac{\theta(e^{-dx} - e^{-dx_0})}{d} \right] \right\}$$

where $\theta = c/a$. The EGRR for this model is $R(x) = ax^{1-b} + cx e^{-dx}$. This cannot be constant over an interval, so power-law behaviour cannot occur. However upper-tail power law behaviour can occur, as in Model I, for values of $b \geq 1$.

The log-likelihood $\ell_2(a, b, \theta, d)$ can be maximized with respect to a analytically, as for Model I, yielding a concentrated log-likelihood

$$\hat{\ell}_2(b, \theta, d) = \sum_{i=1}^n \log(x_i^{-b} + \theta e^{-dx_i}) - n \log \left(\sum_{i=1}^n \left\{ \frac{x_i^{1-b} - x_0^{1-b}}{1-b} - \frac{\theta(e^{-dx_i} - e^{-dx_0})}{d} \right\} \right)$$

which can be maximized numerically to obtain MLEs of b , θ and d and hence MLEs of a and c . Table 2 gives these estimates, while Fig. 6 shows Q–Q plots for this model. The fit for Yosemite is improved considerably and there is some improvement in fit for N.E. Alberta and

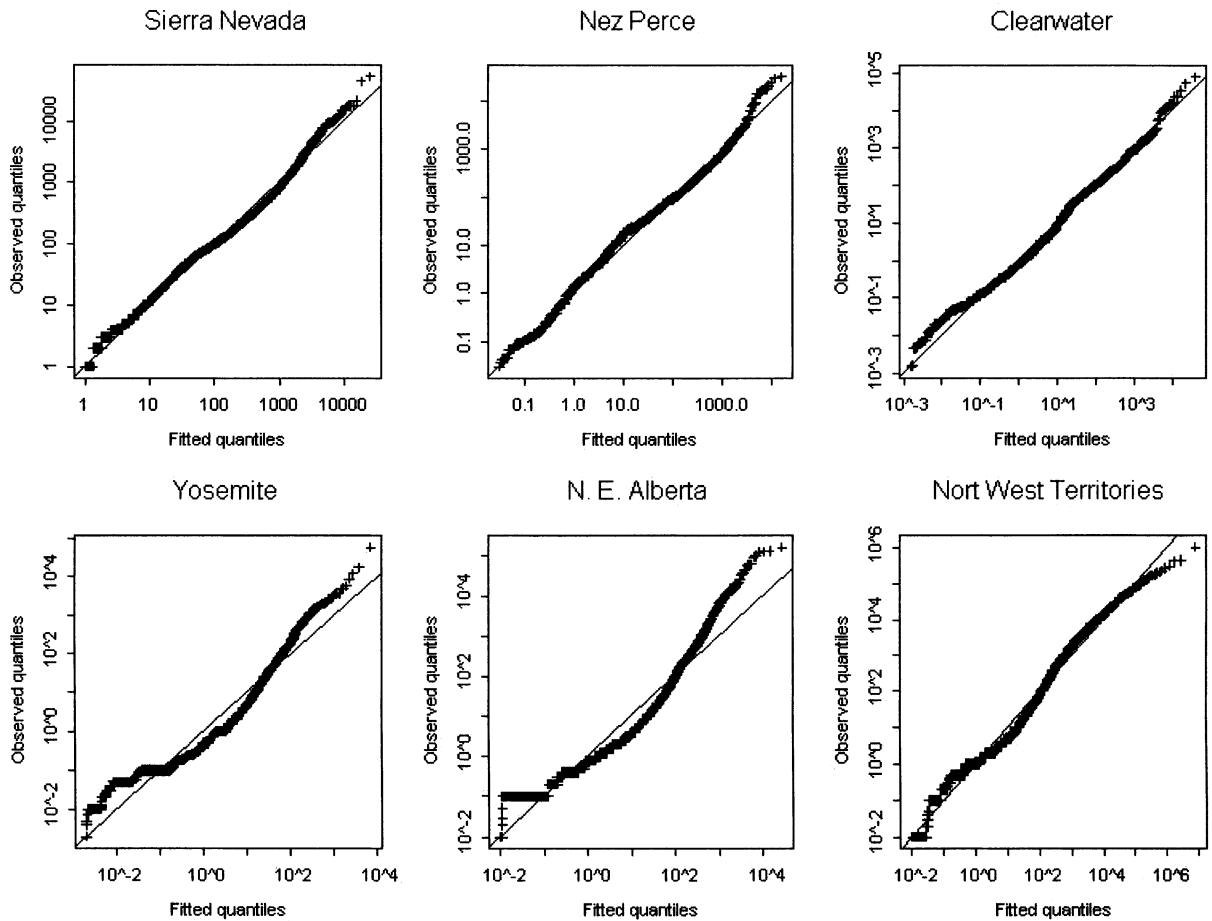


Fig. 5. Q–Q plots showing the quantiles of the observed distribution versus that of the fitted distribution using the Weibull model (Model I), with logarithmic scales on both axes. Systematic departures from the 45° line suggest model lack of fit.

Table 2

Maximum likelihood estimates of the four parameters (a , b , c and d) of the competing hazards model (Model II) with the corresponding maximized log-likelihoods

	\hat{a}	\hat{b}	\hat{c}	\hat{d}	$\hat{\ell}$
Sierra Nevada*	0.0651	0.622	−0.0629	0.616	−33 912.02
Nez Perce*	0.0668	0.601	−0.0239	0.134	−22 756.85
Clearwater	0.0898	0.689	0.275	1.893	−9263.81
Yosemite	0.126	0.681	3.320	2.709	−26 404.20
N.E. Alberta	0.106	0.725	1.196	0.873	−52 396.16
North West Territories	0.117	0.852	0.196	0.413	−27 270.08

* In these two cases the MLE of c is negative. If one restricts c to be positive, $\hat{c} = 0$ in both cases. In this case, the corresponding MLEs of b and the maximized log-likelihood are those given for Model I in Table 1.

Northwest Territories. However, the fitted quantiles for Northwest Territories are still too large, whereas in all of the other cases, they are too small.

4.3. Model III—log Weibull (three parameters)

It is not difficult to show that the hazard-rate function for $Y = \log X$ is related to that for X by $\rho_Y(y) = e^y \rho_X(e^y) = R(e^y)$. Thus, Fig. 3 (apart from the tick marks on the abscissa) gives plots of the hazard rate for Y , $\rho_Y(y)$, (on a log scale) against y . The monotonicity and concavity of these plots suggest that a model of the form $\log \rho_Y(y) = A +$

$b \log(y + c)$ might provide a reasonable fit. This translates to hazard rate functions of the form

$$\rho_Y(y) = a(y + c)^b \text{ and } \rho_X(x) = \frac{a}{x} (\log(x) + c)^b,$$

which is a Weibull hazard for $(Y + c)$, i.e. Y has a pdf of the form

$$f_Y(y) = a(y + c)^b \exp\left[-\frac{a}{b+1} \{(y + c)^{b+1} - (y_0 + c)^{b+1}\}\right]$$

where $y_0 = \log x_0$ and $c > -y_0$. The EGRR is $R(x) = a(\log x + c)^b$. Since this cannot be

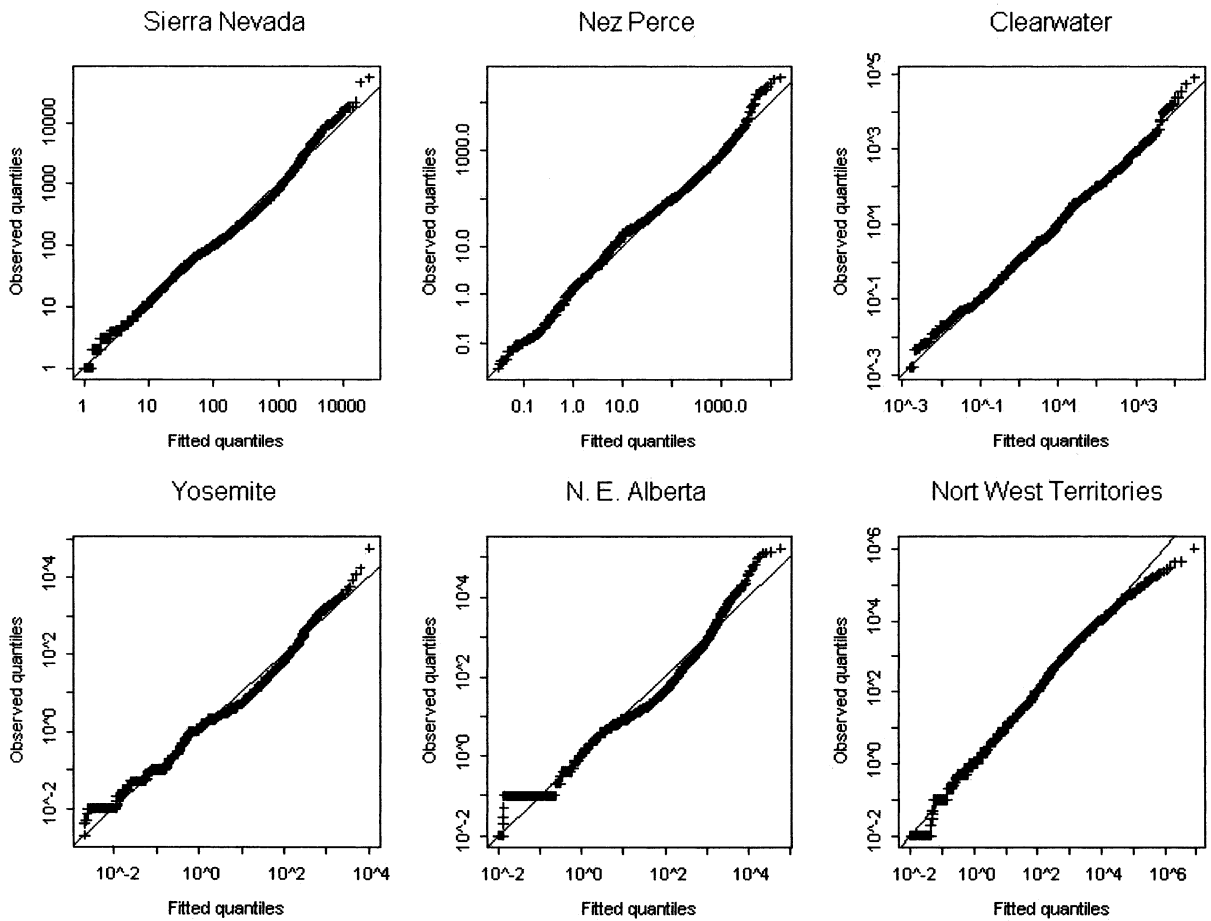


Fig. 6. Q–Q plots showing the quantiles of the observed distribution versus that of the fitted distribution using the ‘competing hazards model’ (Model II), with logarithmic scales on both axes. Systematic departures from the 45° line suggest model lack of fit. Note that if all parameters in the model are constrained to positive values, the plots for Sierra Nevada and Nez Perce should be replaced by the corresponding plots in Fig. 5.

Table 3

Maximum likelihood estimates of the three parameters (a , b and c) of the log-Weibull model (Model III) with the corresponding maximized log-likelihoods

	\hat{a}	\hat{b}	\hat{c}	$\hat{\ell}$
Sierra Nevada	32.13e−5	3.334	3.867	−33 898.28
Nez Perce	0.0041e−5	5.960	10.362	−22 773.63
Clearwater	0.167e−5	4.218	14.227	−9268.48
Yosemite	9583.8e−5	0.737	6.340	−26 208.80
N.E. Alberta	7939.2e−5	0.971	4.748	−52 486.30
North West Territories	7.798e−5	2.587	19.461	−27 383.15

Note that to make the maximized log-likelihood compatible with that for Models I and II, the quantity $\sum_{i=1}^n \log x_i + n \log n - n$ was added to $\hat{\ell}_3(\hat{b}, \hat{c})$. The first term corresponds to the Jacobian for the change of variable from x to $y = \log x$, while the other terms correspond to constants omitted from $\hat{\ell}_1$ and $\hat{\ell}_2$.

constant on an interval, power-law behaviour is not possible. Conditional upper-tail power-law behaviour is not possible.

The log-likelihood $\ell_3(a, b, c)$ for y_1, y_2, \dots, y_n can be maximized analytically over a (as for Model I) and substituted back into ℓ_3 to yield a concentrated log-likelihood

$$\hat{\ell}_3(b, c) = n \log(b + 1) + b \sum_{i=1}^n \log(y_i + c) - n \log \left(\sum_{i=1}^n \{(y_i + c)^{b+1} - (y_0 + c)^{b+1}\} \right).$$

This can be maximized numerically to yield MLEs for b and c and then of a . Table 3 gives these estimates for the six data sets, while Fig. 7 shows Q–Q plots for this model. The fit is very good for the three data sets in the top row, but not so good for those in the bottom row. It is exceptionally good for the Sierra Nevada and Clearwater.

Of the three parametric models considered, there is no single one that provides a best fit for all six data sets. An examination of the values of the maximized log-likelihood suggests that Model III is best for the Sierra Nevada and Yosemite data sets with Model II best for all of the others. However, for the Yosemite data the Q–Q plot for Model III is unsatisfactory, with that for Model II much better. For Sierra Nevada, the Model III Q–Q plot is satisfactory. Overall Model II seems to be the best fitting model. While Model III is better for Sierra Nevada, its superiority over Model II in that single case is only slight.

5. Conclusions

There have been a number of different approaches used to date in the modelling of the size and spread of fires. Models involving the notion of self-organized criticality (Bak et al., 1990; Drossel and Schwabel, 1992; Malamud et al., 1998) assume that fires are part of a class of phenomena (along with avalanches, earthquakes, sandpiles, etc.) which have the property that they occur only above a certain threshold, where positive feedbacks produce a cascade of activity. These models produce power-law relationships between the frequency and size distribution of events. Models used to examine the landscape effects of multiple fires (Baker et al., 1991; Keane et al., 1996; Li et al., 1999) require the fire size distribution as input. Another modelling approach has been to simulate the growth of fires, either using percolation (Beer, 1990; Beer and Enting, 1990) or more complex procedures that involve rules that control probabilities of spread to adjacent pixels on a rasterized landscape (Haydon et al., 2000). Of these approaches, our model is closest to the stochastic simulation approach. However, we have used a birth–death process model for the growth of fires from which a parametric form for the fire-size distribution can be derived analytically.

A careful analysis of actual data and a theoretical investigation into conditions necessary to produce it, suggest that claims of power-law behaviour in the fire-size distribution are exaggerated and that power-law behaviour, at best, only

holds over a limited range of sizes. In this paper, the concept of the extinguishment-growth rate ratio (EGRR) has been introduced and related to familiar statistical concepts, such as the hazard rate and survivor function. It has been shown how a constant EGRR is necessary for power-law behaviour. A constant EGRR occurs in the simple null model in which fires grow at a constant proportional rate (with area growing exponentially in expectation), with constant probability of extinguishment. However, such constant rates would seldom be expected to occur naturally. Away from the null model, a constant EGRR will only occur if both the extinguishment rate and the proportional growth rate depend on size in the

same way. There seems to be no apparent reason why this should be the case and thus, little reason to expect power-law behaviour. Examination of the six empirical area distributions suggests that on the whole the EGRR increases with area and is constant at most over a limited range of sizes for one or two regions.

The EGRR and the hazard rate function can be estimated nonparametrically, from a histogram-based estimate of the density function and these nonparametric estimates can be used to suggest parametric forms for the hazard rate and hence for the density of the distribution of fire size. In the paper, we have discussed three such forms. While none provides a perfect fit to all of the sets

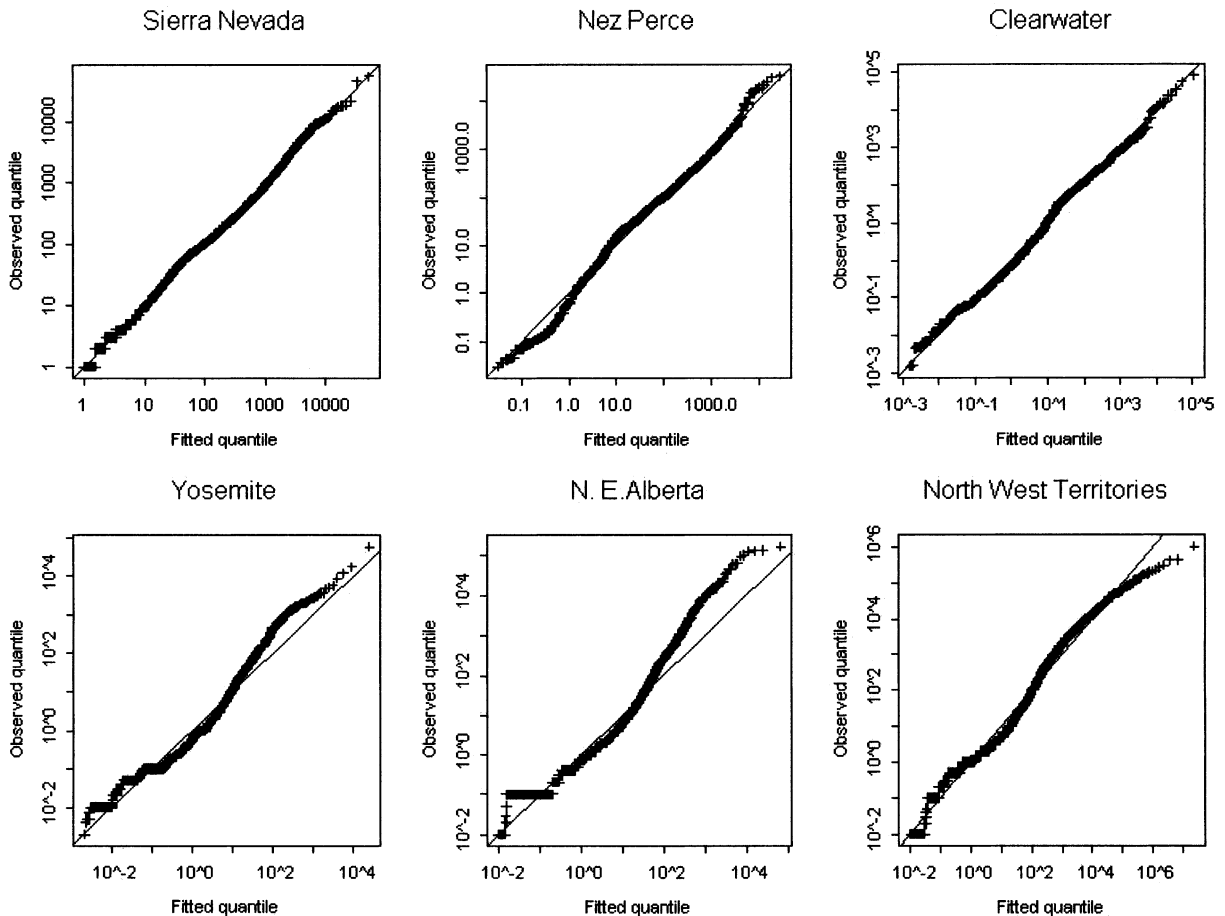


Fig. 7. Q–Q plots showing the quantiles of the observed distribution versus that of the fitted distribution using the log Weibull model (Model III), with logarithmic scales on both axes. Systematic departures from the 45° line suggest model lack of fit.

of data, this is perhaps to be expected given the differences in the terrain, climate and ecology of the six regions. The competing hazards model (Model II) provides a good fit for all but the very largest fires. Such fires are relatively rare, so randomness (sampling error) may be one reason for this. Another concerns the limits (in space and time) that occur for real fires, but which are not included in the model. For fires in the mountainous regions (first four data sets), topographic barriers may slow the rates of growth of large fires, e.g. with fires spreading up mountain slopes they will eventually run into higher elevation areas, which are likely to be wetter and with sparser vegetation, slowing the rate of growth. Eventually, when a fire front reaches a ridge, it may go out. Such behaviour is less likely in the Taiga (Northwest Territories data), with flatter, more uniform terrain. There are temporal barriers as well. The fire season does not last for ever. Eventually, the change of season will result in even the very largest fire being extinguished naturally. It is quite likely that this aspect is most important in the Northwest Territories, while topographic limitations are more important elsewhere. This could explain the fact that the observed size distribution for the Northwest Territories data deviates in the upper tail from the fitted distribution in the opposite direction to that for the other five regions.

The assumption behind the competing hazards model (Model II) is that there can be more than one cause of a fire going out and these causes may operate on different spatial scales. Extinguishment through lack of fuel is likely to be a consideration mainly for small fires, while extinguishment through rain events will be a possibility at all sizes, even though the probability of extinguishment through such a cause may decrease with fire size. The competing hazards model described in Section 4.2 reflects this with the extinguishment rate being the sum of two components, one decreasing rapidly and the other slowly.

Acknowledgements

We gratefully acknowledge the thoughtful comments and suggestions of Barry Hughes (Univer-

sity of Melbourne) concerning the theoretical model. We would also like to thank Steve Cumming (University of Alberta) for directing us to the N.E. Alberta and Northwest Territories data. This paper was written while the first author was visiting the Department of Mathematics and Statistics, University of Melbourne, whose support and hospitality are gratefully acknowledged. The research was supported by NSERC grant OGP 7252.

Appendix A. Derivation of main results

For a continuous random non-negative variable X with pdf $f(x)$, the survivor function is defined as

$$S(x) = P(X \geq x) = \int_x^\infty f(x')dx'$$

while the hazard rate function is defined as

$$\rho(x) = \lim_{dx \rightarrow 0} \left\{ \frac{1}{dx} P(X < x + dx | X \geq x) \right\}$$

It is easily confirmed that

$$S(x) = \exp\left(-\int_{x_0}^x \rho(x')dx'\right),$$

$$f(x) = \rho(x)\exp\left(-\int_{x_0}^x \rho(x')dx'\right),$$

where x_0 is the minimum value that X can assume (i.e. $x_0 = \inf\{x:f(x) > 0\}$) and that

$$\rho(x) = -\frac{d}{dx} \log S(x) = -\frac{S'(x)}{S(x)}$$

We show now that the graph of $\log S(x)$ vs. $\log x$ will be linear (respectively concave, convex) at some point \tilde{x} if $R'(\tilde{x}) = 0$ (respectively, < 0 , > 0) where $R(x) = x\rho(x) = (xf(x)/S(x))$. We have

$$\log S(x) = -\int_{x_0}^x \rho(x')dx'.$$

If $y = \log x$, this can be written

$$\log S(x) = -\int_{x_0}^{e^y} \rho(x')dx'.$$

so that

$$\frac{d}{dy} \log S(x) = -e^y \rho(e^y) = -R(e^y).$$

Thus, $\log S(x)$ is linear, concave or convex in $\log x$ at a point \tilde{x} according to whether $R(x)$ is constant, increasing or decreasing at \tilde{x} .

For the stochastic model described in Section 3, the hazard rate was shown to be of the form $(\rho(x)/\mu(x))$, so that $R(x) = (x\nu(x)/\mu(x))$ which is the ratio of the extinguishment rate $\nu(x)$ to the proportional expected growth rate $\mu(x)/x$. Thus, it is the behaviour of the extinguishment-growth rate ratio (EGRR) which determines whether $\log S(x)$ is linear, concave or convex in $\log x$, which in turn determines whether the distribution of X is behaving as a power law, or is changing faster than, or slower than a power law.

For asymptotic power-law behaviour in the upper tail we require that $f(x) \sim x^{-\alpha-1}$ and $S(x) \sim x^{-\alpha}$ as $x \rightarrow \infty$. This will be met if and only if $\log S(x) \sim -\alpha \log x$ as $\log x \rightarrow \infty$. This condition will certainly be met if $R(x) \rightarrow R_\infty > 0 (x \rightarrow \infty)$; but will not be met if $R(x)$ diverges as $x \rightarrow \infty$, since in this case the slope of $\log S(x)$ against $\log x$ will diverge. The only case that remains to be resolved is when $R(x) \rightarrow 0 (x \rightarrow \infty)$. It is not difficult to show that $R(x) \rightarrow 0$ if and only if $S(x) \rightarrow S_\infty > 0$. In this case, the distribution of X is improper in that there is a nonzero probability ($= S_\infty$) that X is infinite. Clearly in this case asymptotic power-law behaviour cannot occur. However, it is possible that for the conditional distribution of X , given that X is finite, can exhibit power-law behaviour, i.e. that

$$P(X \geq x | X < \infty) = \frac{S(x) - S_\infty}{1 - S_\infty} \sim x^{-\alpha}$$

A necessary and sufficient condition for this is that $R(x) \sim x^{-\alpha}$.

References

- Bak, P., Tang, C., Wiesenfeld, K., 1988. Self-organized criticality. *Phys. Rev. A* 38, 364–374.
- Bak, P., Chen, K., Tang, C., 1990. A forest-fire model and some thoughts on turbulence. *Phys. Lett. A* 147, 297–300.
- Baker, W.L., 1989. Landscape ecology and nature reserve design in Boundary Waters Canoe Area. *Ecology* 70, 23–35.
- Baker, W.L., Egbert, S.L., Frazier, G.F., 1991. A spatial model for studying the effects of climatic change on the structure of landscapes subject to large disturbances. *Ecol. Model.* 95, 145–164.
- Barndorff-Nielsen, O., 1977. Exponentially decreasing distributions for the logarithm of particle size. *Proc. R. Soc. Lond. A* 353, 401–419.
- Beer, T., 1990. Percolation theory and fire spread. *Combust. Sci. Tech.* 72, 297–304.
- Beer, T., Enting, I.G., 1990. Fire spread and percolation modelling. *Math. Comput. Model.* 13, 77–96.
- Berman, S.M., Frydman, H., 1996. Distributions associated with Markov processes with killing. *Commun. Stat.-Stoch. Models* 12, 367–388.
- Cumming, S.G., 2001. A parametric model of fire-size distribution. *Can. J. For. Res.* 31, 1297–1303.
- Drossel, B., Schwabel, F., 1992. Self-organized critical forest-fire model. *Phys. Rev. Letts.* 69, 1629–1632.
- Haydon, D.T., Friar, J.K., Pianka, E.R., 2000. Fire driven mosaics in the Great Victoria Desert, Australia. IIA spatial and temporal landscape model. *Landsc. Ecol.* 15, 407–423.
- Keane, R.E., Morgan, P., Running, S.W., 1996. FIRE-BGC—A mechanistic ecological process model for simulating fire succession on coniferous forest landscapes of the northern Rocky Mountains. USDA Forest Service, Intermountain Research Station, Research paper INT-RP-484, 122p.
- Li, C., Corns, I.G.W., Chang, R.C., 1999. Fire frequency and size distribution under normal conditions: a new hypothesis. *Landsc. Ecol.* 14, 533–542.
- Malamud, B.D., Morein, G., Turcotte, D.L., 1998. Forest fires: an example of self-organized criticality. *Science* 281, 1840–1842.
- McKelvey, K.S., Busse, K.K., 1996. Twentieth-century fire patterns on forest service lands. Sierra Nevada Ecosystem Project: Final Report to Congress, vol. II. Assessments and Scientific Basis for Management Options. Davis, University of California, Centers for Water and Wildland Resources.
- Ricotta, C., Avena, G., Marchetti, M., 1999. The flaming sandpile: self-organized criticality and wildfires. *Ecol. Model.* 119, 73–77.
- Silverman, B.W., 1986. *Density Estimation for Statistics and Data Analysis*. Chapman and Hall, London.
- Tuckwell, H.C., 1988. *Elementary Applications of Probability Theory*. Chapman-Hall, London.